SUbsonic Single Aft eNgine (SUSAN) System Integration Analysis with the Future Aircraft Sizing Tool (FAST)

Yi-Chih Wang*, Miranda Stockhausen*, Paul R. Mokotoff*, Maxfield Arnson*, and Gokcin Cinar†
Department of Aerospace Engineering, University of Michigan, Ann Arbor, Michigan, 48109, USA

NASA proposed the SUbsonic Single Aft eNgine electrofan concept (SUSAN) to meet the increasing demand for electrified aircraft designs, which has the potential to reduce CO_2 emissions by 50% and limit aviation's environmental impact. SUSAN's propulsion system consists of one turbofan engine and sixteen distributed electric propulsors. It is designed as a commercial transport that carries a 180-passenger payload for 2,500 nautical miles, while cruising at Mach 0.785 and 37,000 ft. SUSAN's design includes multiple advanced technologies, such as a single aft engine with boundary layer ingestion, distributed electric propulsion system, and several state-of-art electric subsystems. This paper integrates various technologies and methods developed for SUSAN within a single modeling and simulation environment. SUSAN is modeled using the Future Aircraft Sizing Tool (FAST) developed by the University of Michigan. Using aircraft specifications and a design mission profile gathered from literature, FAST evaluates the system-level feasibility and performance of SUSAN and its integrated technologies. Additional propulsion system and BLI models are introduced to incorporate SUSAN's advanced technologies into its design. The resulting SUSAN model has an MTOW of 189,394 lbm, an OEW of 117,460 lbm, and a predicted block fuel burn for the design mission of 30,701 lbm. The SUSAN model has a high lift to drag ratio of 20.49, encouraging further investigation into how these advanced technologies can reduce dependency on control surface sizing and improve aircraft efficiency overall. FAST predicts the cruise TSFC for the aft engine 0.4372 lbm/(lbf · hr), which includes the effects of BLI technology.

I. Nomenclature

BLI	=	Boundary-Layer Ingestion
CR	=	Cruise
DEP	=	Distributed Electric Propulsion
EAP	=	Electrified Aircraft Propulsion
EG	=	Electric Generator
EM	=	Electric Motor
EPFD	=	Electrified Powertrain Flight Demonstration
EPS	=	Electric Power System
ES	=	Energy Source
FAA	=	Federal Aviation Administration
FAST	=	Future Aircraft Sizing Tool
GHG	=	Greenhouse Gas
HEATheR	=	High-Efficiency Electric Aircraft Thermal Research
HEMM	=	High-Efficiency Megawatt Motor
HPS	=	High-pressure shaft
KPPs	=	Key Performance Parameters
LAHX	=	Liquid/Air Heat Exchanger
LPS	=	Low-pressure shaft
L/D	=	Lift to drag ratio

*Graduate Student Research Assistant, Department of Aerospace Engineering, University of Michigan, Ann Arbor, Michigan 48109, AIAA Student Member
†Assistant Professor, Department of Aerospace Engineering, University of Michigan, Ann Arbor, Michigan 48109, AIAA Senior Member.

NLF	=	Natural laminar flow
PS	=	Power Source
SLS	=	Sea-level static
TET	=	Turbine entry temperature
TOC	=	Top-of-Climb
STARC-ABL	=	Single-Aisle Turboelectric Aircraft with Aft Boundary Layer Propulsion
SUSAN	=	SUbsonic Single Aft eNgine
TS	=	Thrust Source
TSFC	=	Thrust Specific Fuel Consumption

II. Introduction

With increasing public awareness of global warming and greenhouse gas (GHG) emissions, governments and regulatory groups are planning sustainable development strategies for the coming decades. The U.S. Aviation Climate Action Plan targets net-zero GHG emissions from the aviation sector by 2050. The Federal Aviation Administration (FAA) will analyze the CO_2 emissions of the current and future domestic and international aviation demands with plans to build a net-zero sustainable aviation system [1]. NASA is collaborating with the FAA, industry, and academia to achieve this goal by 2050. NASA's SUbsonic Single Aft eNgine (SUSAN) electrofan concept harnesses a 20 MW electrified aircraft propulsion (EAP) system. Its partially turboelectric propulsion architecture and advanced propulsion airframe integration improves efficiency and reduces flight CO_2 emissions by 50% [2]. SUSAN is a regional transport aircraft with a 2,500 nautical mile (nmi) design mission and 750 nmi economy mission, and carries 180 passengers at a nominal cruise altitude and speed of 37,000 ft and Mach 0.785, respectively [2, 3]. SUSAN's design also includes boundary-layer ingestion (BLI) technology in the aft turbofan engine, along with a T-tail [4] and two distributed electric propulsion (DEP) arrays, shown in Fig. 1. Each DEP array consists of eight electric propulsors in mail-slot nacelles mounted beneath the wings. Each propulsor is comprised of two electric motors powering two counter-rotating ducted fans.

Fig. 1 The Subsonic Single Aft Engine (SUSAN) aircraft concept, published by NASA [5].

A literature review of EAP illustrates how BLI and DEP technologies individually reduce the energy costs associated with conventional aviation. Yildirim et al. [6] determined that in the Single-Aisle Turboelectric Aircraft with Aft Boundary Layer Propulsion (STARC-ABL), the application of turboelectric propulsion and BLI reduced required power by 10-15% at cruise to achieve the same net body force coefficient relative to a reference aircraft with podded propulsors. At low altitudes and speeds, the power savings was reduced to 5-8%. An investigation from Machado et al. [7] established that the DEP design provided a 22.2% drag savings and 1.3% shaft power savings compared to a conventional underwing-mounted configuration with dual podded propulsors. The benefits result from a lower fan

pressure ratio for the DEP array and reduced thrust-induced drag. These studies suggest that the integration of BLI and DEP could yield further benefits when applied to the SUSAN aircraft.

The SUSAN aircraft is powered by a single fuel-burning turbofan engine, which is integrated into the aft fuselage. The propulsion system is shown in Fig. 2. The engine is designed to contribute 35% of the total cruise thrust while simultaneously powering four 5 MW main generators connected to the low pressure shaft, and one 1 MW generator turbine control generator attached to the high pressure shaft. The main generators transmit power to the 16 electric propulsors, providing the remaining 65% cruise thrust [8].

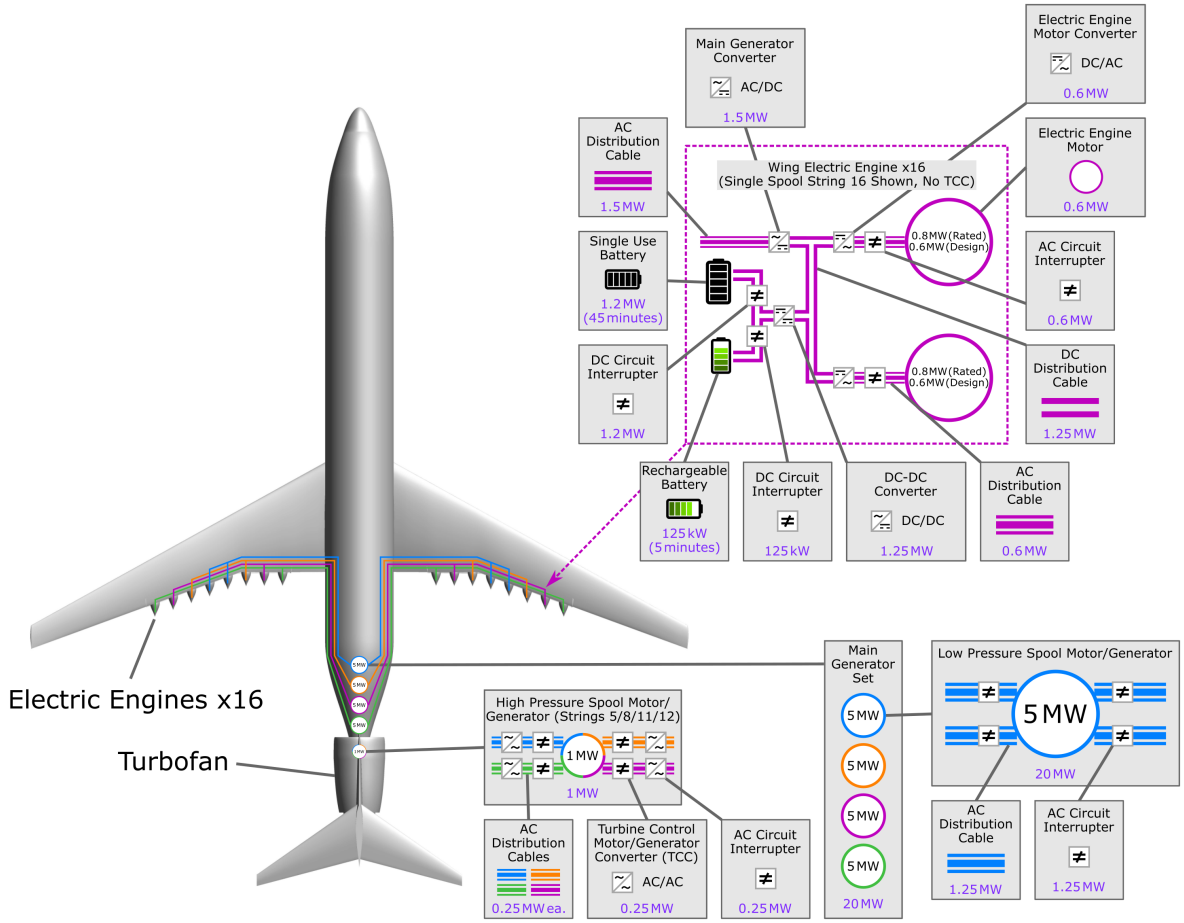

Fig. 2 SUSAN's propulsion system integrated into the aircraft [9].

Each electric propulsor includes two fans driven by two 0.6 MW counter-rotating electric motors and a 125 kW rechargeable battery rated for a 5-minute discharge. The battery helps stabilize the power demand in the propulsion system, provides a temporary power boost, and supports rapid electric motor response during acceleration. Additionally, the propulsion system includes a 1.2 MW single-use battery to allow for a 45-minute, 300 nmi flight in case of a turbofan engine failure [2, 9].

The electric propulsors are mainly driven by the low-pressure shaft (LPS) (90% of its power) with a small amount from high-pressure shaft (HPS) (10% of its power), which can reduce the size of the electric systems [10]. The pressure ratios are assumed to be 1.37 for the fan, 1.25 for the wing fans, and 3.1 for the low-pressure compressor. The overall pressure ratio (OPR) for the SUSAN turbofan is 86 [7, 9]. Additionally, Chapman et al. [9] indicated that the effective bypass ratio would be over 20 when considering the wing propulsors and fan air bypassing the core engine, compared to 5.66 with only fan air. Following the literature, the efficiency of the wing fans are assumed to be 96% [9]. The aft engine fan, low and high-pressure compressors, and turbine efficiencies are assumed to be between 90 and 92%. These efficiencies correspond to an approximate cruise thrust specific fuel consumption (TSFC) of 0.43 lbm/(lbf*hr).

In the electric power system (EPS), a high-efficiency megawatt motor (HEMM) is used for each electric motor and generator. The HEMM's self-cooling and superconducting technology allows it to reach a high specific power (16 kW/kg) and efficiency (99%) without an external cooling system [11, 12]. To stabilize the battery voltage output and match the electric components' different voltage levels, the EPS DC-DC converters are based on the High-Efficiency Electric Aircraft Thermal Research (HEATheR) design and incorporated into the model. These yield a high efficiency (98.6%) and high power density (20 kW/kg), reduce the HEMM rotor loss, and only generate 5% heat loss. This represents a significant technological improvement over current state-of-the art components, which have a heat loss of 20% [9, 13–15]. For the wiring, Dever et al. [16] identified its key performance parameters (KPPs) – including the specific weight and length-specific power loss at different operating currents – and developed a model of the wiring mass and KPPs for EAP systems.

The nominal mission profile includes a 2,500 nautical mile design mission, along with the required reserve mission segments (a diversion and hold). Since SUSAN and the Boeing 737-8 Max are designed for similar payload and range requirements, the CFM LEAP-1B25 engine from the 737-8 Max is set as the baseline engine in this analysis. The propulsion system is sized for 11,500 lbf of thrust at the top of the climb, 7,134 lbf of thrust for cruise, and 54,300 lbf of thrust for takeoff [2, 8]. The power required for the Boeing 737-8 Max is 9.2 MW for level flight and 12.2 MW for climb. These power demands were used along with estimates of future technological capacities to set the mission segment power requirements of 10 MW in cruise and 20 MW in climb [8, 17, 18].

Based on the literature reviews and mission design, this paper aims to model the SUSAN concept and perform a system-level analysis of the integrated concept. This will be achieved by consolidating the novel engine, electrified propulsion system, and technologies and subsystems together within a single modelling and sizing platform. The Future Aircraft Sizing Tool (FAST) [19] is used for this investigation. FAST is an aircraft sizing tool for fixed-wing aircraft of any propulsion architecture, created under NASA's Electrified Powertrain Flight Demonstration (EPFD) program, and has been released as open-source software*. Fig. 3 shows the high-level computational procedure within FAST, highlighting the pre-processing, sizing, and mission analysis modules. Its rapid aircraft sizing and analysis capabilities allow for early-phase conceptual design, and is useful for design space exploration and sensitivity analyses. Visualizations of the aircraft configuration being analyzed are also provided to help engineers quickly evaluate the design decisions made. In this work, FAST is leveraged to unify the advanced technologies previously studied from literature into one, comprehensive SUSAN model, and determine the system-level benefits and feasibility of its design.

FAST can model SUSAN's benefits in the following two ways. First, DEP, NLF, and BLI effects are represented by increases in lift-drag (L/D) ratio. Second, the unconventional propulsion architecture is modeled using interdependency matrices (further explained in Section III.C). FAST allows the rapid comparison of off-design analyses of the sized SUSAN model with different combinations of advanced technologies to evaluate the system-level impact of their use [19]. These results can be analyzed for changes in control surface sizing, fuel flow behavior, and more to investigate the integrated benefits of SUSAN's technological improvements. FAST's use of historical databases and regressions help to reduce the potential error inherent to modeling advanced propulsion systems with many unknowns [20], making it a powerful tool for comparative design analyses.

This paper will explain the technical approach used to develop the SUSAN model, including the computational tools and required components. It will explain the design of the propulsion and engine systems for the SUSAN aircraft model, including necessary architecture simplifications and the thrust sizing for the EAP system. The approach taken to apply advanced technologies will also be discussed. Next, the results of the SUSAN model aircraft sizing and performance analysis will be presented and discussed. Particular attention will be paid to the implications of these results for the block fuel requirements and traditional control surface sizing. Finally conclusions and aims for future development of the model will be drawn based on the lessons learned from these initial results.

III. Technical Approach

To model SUSAN, FAST requires an aircraft specification file to describe the aircraft's design and key performance parameters, and a mission profile specification file to describe the mission profile that the aircraft flies. These files were created by using data from a literature review of SUSAN's design specifications published by NASA since 2021 [21–23] and are discussed in detail next. Any unknown design or key performance parameters for SUSAN were approximated using standards and averages from known single-aisle passenger jets of a similar weight class to the Boeing 737 Max. One performance parameter with limited public data were the airspeeds along the mission profile. Available airspeed data for commercial aircraft is generally sparse, so the FAA speed limits for different altitude zones were used to define

*https://github.com/ideas-um/FAST

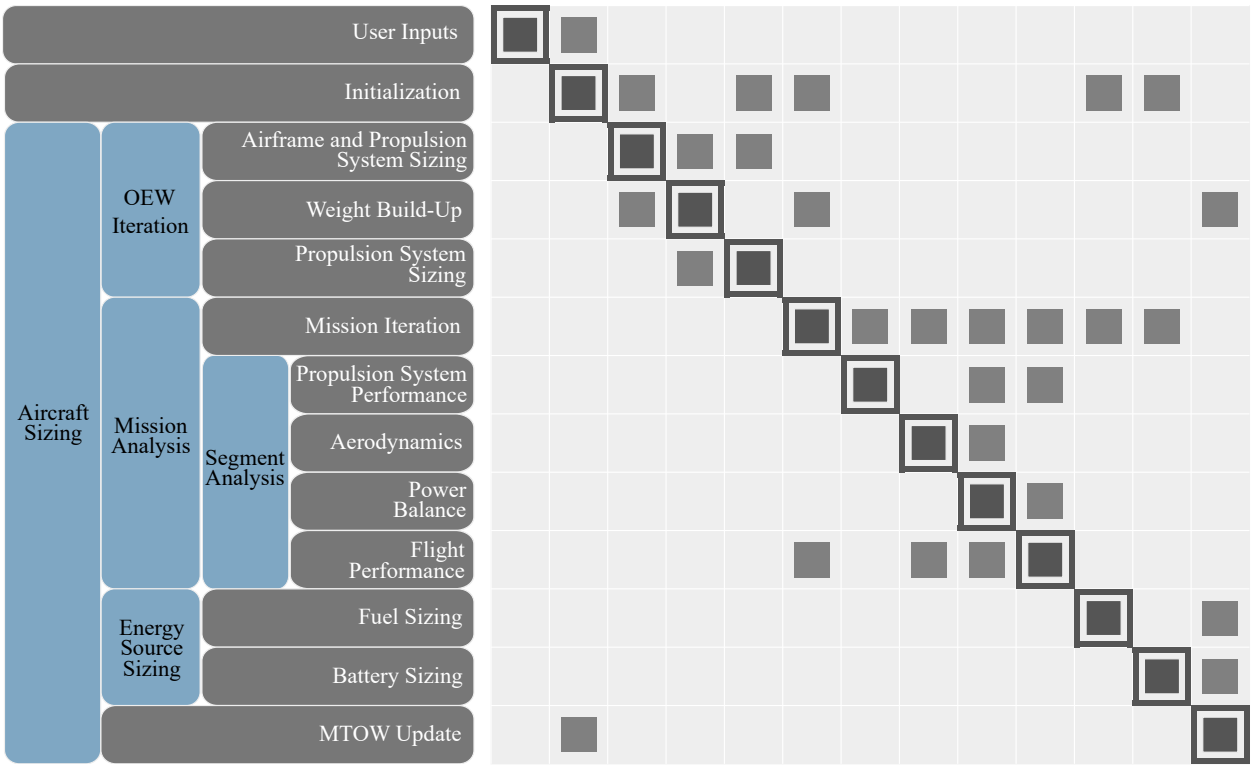

Fig. 3 Aircraft analysis workflow within FAST [19].

the airspeed schedule for the mission profile. These inputs are discussed in more detail throughout the next section.

A. Aircraft Specifications

The aircraft specification file contains information about the aircraft's design and performance parameters. Table 1 lists the parameters used to model SUSAN in FAST. The weights provided serve as an initial guess to start the aircraft sizing iteration. These values, and additional estimates for aircraft weights and design mission performance were collected from previous works done on SUSAN [21, 24]. Those inputs not set in the aircraft specification file were estimated using Gaussian Process Regression models in FAST [20].

Certain values in Tab. 1 were calculated from existing data. For example, the electric motor and generator weights were calculated from their specific energies and required power outputs from existing literature [21]. Wing loading, power, and thrust-weight ratios were all calculated based on the initial MTOW estimate from Chau and Duensing [21]. For a wing area of 1470 square feet and MTOW of 190,890 lbs, the resulting wing loading is 19.7. The SLS thrust and power loading values, respectively, were determined to be 0.298 and 0.378 kW/kg.

The EAP weight was calculated based on the power outputs and power-weight ratios developed in previous SUSAN sizing studies [21]. Since FAST is an early-phase conceptual design tool, components like the thermal management system, wires, and cables are not accounted for in the propulsion system weight. These weights were entered as separate EAP weight variables, as previously shown in Tab. 1. For reference, the EAP component weights are provided in Tables 8 and 9 in Appendix VII.B. SUSAN's single-use and rechargeable batteries were also included in this weight, because they only provide power during the off-design engine failure condition. This separation allows for comparisons between the analysis in FAST and those of previous studies that used more granular analyses. It also preserves the program's ability to size the electric machines for the design mission.

Another value from literature that was adjusted for consistency was the number of passengers carried onboard. It is common to determine the number of passengers by dividing the total payload by a consistent mass ratio per passenger. The analysis from Chau et al. assumed a passenger mass of 100 kg per passenger for a passenger count of 180 [21]. FAST assumes a passenger mass of 95 kg, which increases this maximum passenger load to 190.

Table 1 Specifications and settings for SUSAN model in FAST

Required Inputs		**Weights**	
Engine Class	Turbofan	MTOW, kg	86,586
Passengers	190	Block Fuel, kg	4,722
Range	2,500 nmi	Electric Motor, kg	1,833
Propulsion Architecture	"O"	EAP Weight, kg	11095
Engine Count	1	**Propulsion**	
Top Level Requirements		SLS T/W	0.298
Entry into Service	2040	SLS Thrust, kN	240.2
Performance		**Power**	
Takeoff speed, m/s	82.3	Fuel specific energy, kWh/kg	12
Cruise speed, Mach	0.775	EM efficiency	0.97
Takeoff altitude, m	0	Engine P/W, kW/kg	0.378
Cruise altitude, m	10,668	EAP P/W, kW/kg	10.63
Aerodynamics			
Cruise L/D	19.7		
Wing Loading, Pa	634		

B. Mission Profile

The mission profile specification file contains information about the mission "targets" – a distance- or time-based value that specifies the necessary range or endurance that the aircraft fly – and the mission "segments" – the takeoff, climb, cruise, descent, and landing segments that describe how the aircraft must fly. In addition to the describing the type of segment (takeoff, climb, cruise, etc.), the user prescribes a set of initial and final altitudes and airspeeds for each segment, which serve as the boundary conditions for the mission analyses. The user can also set rates of climb/descent for each segment or allow them to be determined by the mission analysis. The mission targets and segment definitions for SUSAN are described in Tab. 2. The mission profile targets were designated based on the mission profile described by Denham et al. [8] and include:

- **Design Mission:** 2,500 nmi range
- **Diversion:** 100 nmi range
- **Hold:** 45 minute loiter

SUSAN typically cruises at 37,000 feet and Mach 0.785. Chau et al. [21] modified the cruise altitude to 35,000 ft and airspeed to Mach 0.775, which reduces the fuel burn during cruise [21]. For consistency, the modified cruise conditions are included in this study. The climb schedule airspeeds were set based on FAA speed limits at the 10,000 feet ceiling and for holds below 6001 ft [25, 26].

The climb schedule has three segments. First, the aircraft completes the initial climb from takeoff to 1,500 ft and accelerates to 250 kts. After this, SUSAN climbs at 250 kts until the FAA speed limit ceiling at 10,000 ft. Finally, SUSAN completes an accelerated climb to the design cruise conditions. The descent is compressed into a single segment to reduce the computational cost, especially since it has no impact on the propulsion system sizing.

Following descent, the aircraft must be able to fly two FAA required reserve missions. The first is a missed approach. Once the aircraft descends to an altitude of 100 ft, it must go-around and climb to 15,000 ft and accelerate to Mach 0.5 for the second reserve mission, a 100 nmi diversion. Then, SUSAN descends to 1,500 ft and enters a holding pattern for 45 minutes [24].

The boundary conditions for each segment are provided in Tab. 2. The entire mission profile is shown in Fig. 4, which was produced by the IDEAS lab team based on the mission profile information from the 2023 update by Denham et al. [8].

C. Propulsion System Modeling

The components within SUSAN's propulsion system can be generalized into three groups – energy sources (ES), power sources (PS), and thrust sources (TS) – as proposed by Cinar et al. [27]. Energy sources store energy to be used

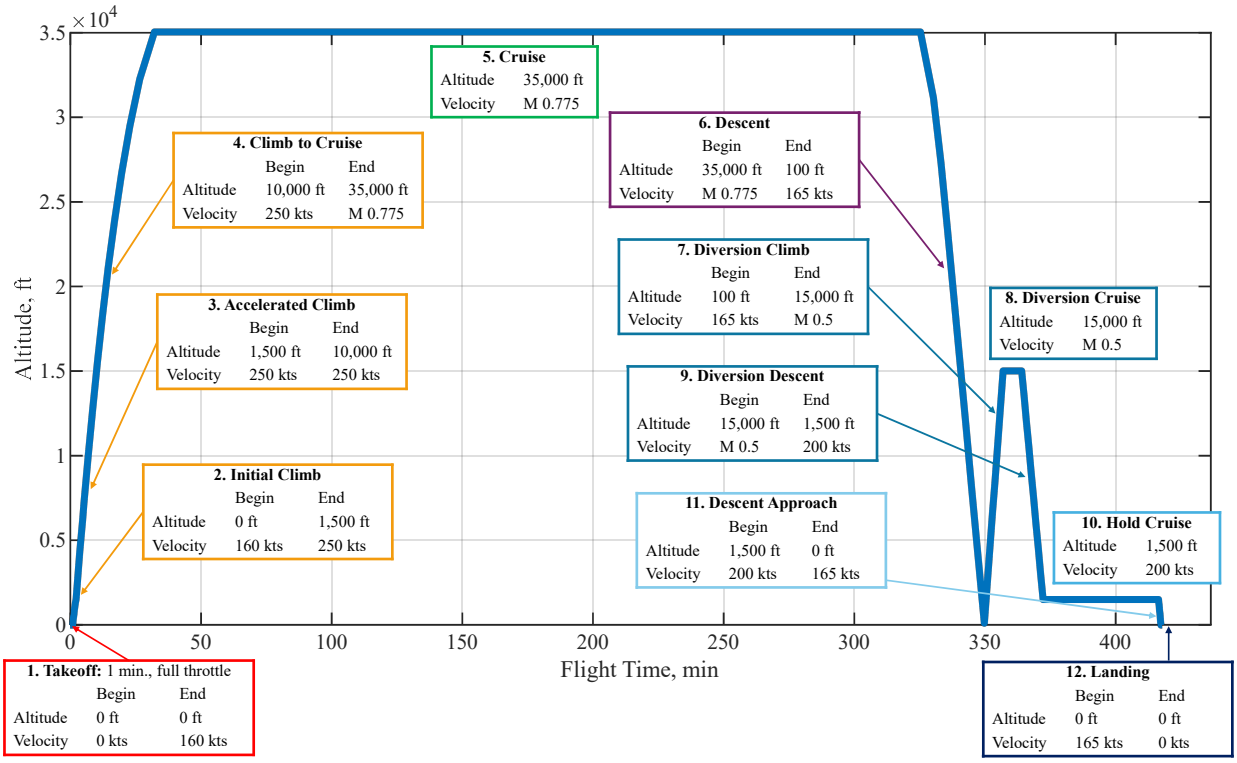

Fig. 4 The nominal mission profile for the SUSAN concept.

by the aircraft. SUSAN's only energy source is jet fuel. Power sources transmit power to other components in the propulsion system architecture. SUSAN's power sources are the turboshaft engine, the electric generators (EG), and the electric motors (EM). Thrust sources generate thrust and propel the aircraft. SUSAN's thrust sources are the large aft fan and 32 ducted fans distributed along the wings. Typically, a turboshaft engine powering a large ducted fan is called a turbofan engine. However, these components are decoupled in the electrified propulsion architecture. This is because the turboshaft engine powers one thrust source, the aft fan, and also transmits power to the four EGs. Each EG transmits power to four electric propulsors. Each electric propulsor is comprised of two EMs turning two wing fans. This powertrain configuration is visualized in Fig. 5.

One limitation of FAST's existing propulsion system architecture framework is that it cannot currently model propulsion systems with more than two power sources arranged consecutively (i.e. in series). As a result, the sequential connection between the turboshaft engine, electric generator, and electric motors must be simplified. This was accomplished by lumping the electric generators and motors together, defining them as an "electric machine", and modeling them with an efficiency that accounted for both components' performance. These electric machines act as power sources and provide power to the 32 distributed wing fans.

To mathematically represent the connections between thrust sources, power sources, and energy sources, this paper implements the interdependency matrices introduced by Cinar et al. [27]. These matrices represent logical maps which store component connections as Boolean values. A 1 represents a connection between components and a 0 represents no connection between the components. There are three interdependency matrices:

1. Thrust source from power source matrix (B_{TSPS}): represents which thrust sources (in rows) are directly connected to the power sources (in columns).
2. Driven power source from driving power source matrix (B_{PSPS}): represents which driven power sources (in rows) are directly connected to the driving power sources (in columns). For SUSAN, the turboshaft engine is a driving power source and the electric machines are driven power sources, because the turboshaft engine powers the electric machines.
3. Power source from energy source matrix (B_{PSES}): represents which power sources (in rows) are directly connected to the energy sources (in columns).

Table 2 Detailed settings of SUSAN design mission in FAST

Mission Segment	Mission ID	Beginning Altitude, ft	Ending Altitude, ft	Beginning Airspeed	Airspeed Type	Ending Airspeed	Airspeed Type
Takeoff	1	0	0	0	Mach	160 kts	EAS
Initial Climb	1	0	1,500	160 kts	EAS	250 kts	EAS
Accelerated Climb	1	1,500	10,000	250 kts	EAS	250 kts	EAS
Climb to Cruise	1	10,000	35,000	250 kts	EAS	0.775	Mach
Cruise	1	35,000	35,000	0.775	Mach	0.775	Mach
Descent	1	35,000	100	0.775	Mach	165 kts	EAS
Diversion Climb	2	100	15,000	165 kts	EAS	0.5	Mach
Diversion Cruise	2	15,000	15,000	0.5	Mach	0.5	Mach
Descent	2	15,000	1,500	0.5	Mach	200 kts	EAS
Hold Cruise	3	1,500	1,500	200 kts	EAS	200 kts	EAS
Descent Approach	3	1,500	0	200 kts	EAS	165 kts	EAS
Landing	3	0	0	165 kts	EAS	0	Mach

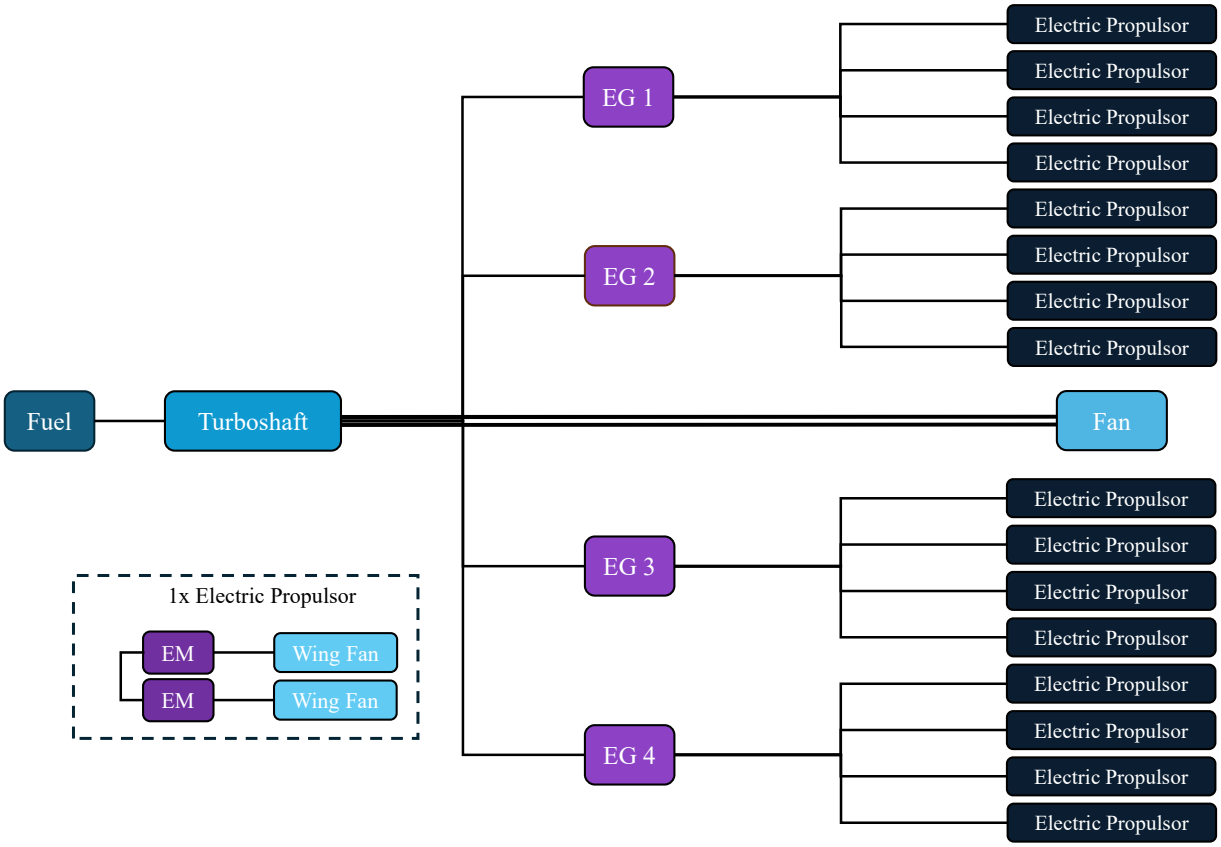

Fig. 5 The powertrain architecture of SUSAN concept.

In addition to the interdependency matrices, a thrust-split matrix is required to quantify the percentage of total thrust produced by each individual thrust source. At cruise, 35% of thrust is provided by the fan and the remaining 65% is provided by the 16 electric propulsors (32 wing fans). Therefore, each electric fan creates $65\%/32$ thrust. The 1×33 thrust-split matrix is provided in Eq. 1. The first entry in the matrix is the fan's thrust contribution, and the remaining ones are the wing fans' thrust contribution.

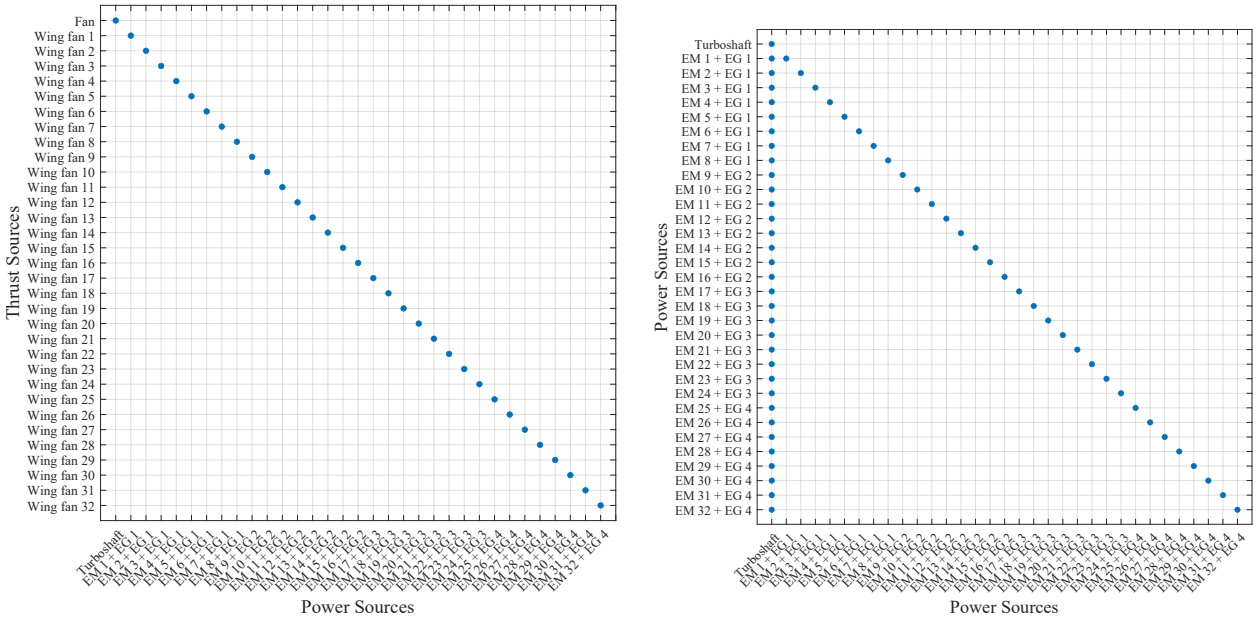

(a) The power transmission from PS to TS, B_{TSPS}. **(b) The power transmission from PS to PS, B_{PSPS}.**

Fig. 6 The powertrain architecture matrices of SUSAN concept.

$$TS = \left[35\%,\ \frac{65\%}{32},\ \frac{65\%}{32}, ...,\ \frac{65\%}{32}\right]_{1\times 33} \tag{1}$$

In the B_{TSPS} matrix, the first row represents the aft fan and the remaining ones represent each of the wing fans. The first column of the matrix is the turboshaft engine. The remaining columns represent the electric machines used to power each ducted wing fan. The turboshaft engine only directly powers one thrust producer, the aft fan. Thus, the first entry in the turboshaft column is 1 and is shown by a blue dot. The remaining entries in the column are 0s, and remaining blank. Each electric machine powers one wing fan, so each respective column has one connection, represented by the blue dots along the diagonal in Fig. 6a.

In the B_{PSPS} matrix, the rows and columns both represent power sources. The first row/column represents the turboshaft engine and the others represent the electric machines. Using the convention set forth by Cinar et al. [27], all power sources power themselves, as shown by the blue dots on the main diagonal in Fig. 6b. Since the turboshaft engine drives all of the electric machines, blue dots are also included throughout the first column of the B_{PSPS} matrix.

Lastly, for the B_{PSES} matrix, there is only one energy source. Thus, the matrix is a column vector with thirty-three rows. In SUSAN, fuel only flows to the turboshaft engine. Therefore, the first entry is a 1 and all others are 0. This matrix is provided in Eq. 2.

Using the matrices defined in this section, SUSAN's propulsion system can be easily modeled in FAST, and its performance can be rapidly assessed.

$$B_{PSES} = [1,\ 0,\ 0, ...0]^T_{33\times 1} \tag{2}$$

D. Propulsion System Sizing

In past analyses involving SUSAN, there is no consensus on how the propulsion system is sized [4, 21, 22, 24]. Recent literature stated that the sizing point is top of climb (TOC) with a required thrust of 4,025 lbf and the electric propulsion system is sized for a 10 MW load [4]. However, the gas turbine engine needs output a load larger than 10 MW to power the EPS and the fan. This is an important consideration when comparing the TSFC estimated by FAST to those in literature, particularly at TOC. For comparison, the Boeing 737-8 Max is taken as a baseline, which requires 12.2 MW at TOC, where 65% of the power is used for electric propulsion [8]. The engine model in FAST was validated by comparing the estimated TSFC to that from literature and ignoring BLI effects (which are added later). The

turbine entry temperature (TET) is required for the engine analysis in FAST but is not specified in literature. A TET was selected by varying it until the TSFC prediction from FAST matched the one from literature. Table 3 shows the SUSAN's gas turbine modeling parameters, where Tab. 3a shows the input values while Tab. 3b shows FAST's outputs.

FAST also outputs an engine weight based on takeoff thrust using a regression. Since SUSAN's propulsion architecture is novel, there is no data available for engine weight estimates involving propulsive power off takes. It is unrealistic to estimate the engine weight solely based on the thrust the gas turbine produces to power the fan – this ignores the power supplied to the EPS and DEP. To generalize the engine weight estimation for all conventional or electrified systems, FAST's regression uses the total SLS thrust (whether produced directly by a fan or electrically via motor) to estimate the engine weight. That way, the regression is not dependent on the propulsion architecture, and accommodates EAP systems that supplement/siphon power to/from the engine.

Table 3 Gas turbine sizing.

(a) FAST's inputs for the SUSAN turbofan.

Input Parameter	Value	Units
Altitude	11,277 [8]	m
Mach Number	0.785 [8]	–
Gas Turbine Thrust (TOC)	17,903** [8]	N
TET	1,978	K
Electrical Off-take (TOC)	7.93** [8]	MW

**The value of gas turbine thrust (TOC) is 35% thrust split of 51,154 N total thrust requirement, and the electrical off-take (TOC) is 65% of 12.2 MW total power requirement [8].

(b) FAST's TSFC prediction for the SUSAN turbofan at the start of climb, including thrust produced by both the gas turbine and the electric propulsors.

Output	FAST	Literature	Difference
TSFC (1/hr)	0.4421	0.4420 [9]	+ 0.02%

There is a significant difference between the engine weight that FAST predicted and the one reported in literature [21]. The number from literature was calculated using WATE++, an established engine weight estimation software. However, it appears that the thrust WATE++ is using to predict engine weight was set at 54,000 lbs, which was the reference thrust value taken from a similarly sized aircraft, the Boeing 737-8 [8]. This is inconsistent with the SUSAN's takeoff thrust, calculated using $T_{\text{SLS}} = \frac{T}{W} \times MTOW$, which is 56,885 lbf, according to recent literature [21]. This suggests that the previous engine weights reported may be an underestimate of the actual engine weight required to power the EAP system.

One possible reason for such a discrepancy could be due to implicit assumptions within FAST. In FAST, historical data from conventional engines is used to predict an engine weight from its required SLS thrust. This prediction is inherently biased against engines which are integrated into an aircraft's airframe, and assumes that any thrust produced by the EPS has the same efficiency losses as mechanical connections. These assumptions cannot be corrected with FAST's existing capabilities because either additional data is needed or a correction factor for integrated propulsion system weights must be implemented into FAST.

Figure 7 graphically compares FAST's engine weight estimate and SUSAN's actual engine weight relative to the historical engine weight data stored in FAST's database [28]. Historical data is shown for large engines producing SLS thrust similar to SUSAN, as well as smaller engines which produce thrusts similar to *half* of what SUSAN requires. The smaller engines' thrusts and weights are doubled to show the engine weights required to produce similar thrust with 2 smaller engines as opposed to one larger engine. As seen from Fig. 7, 2 smaller engines will weigh more than one large engine for the same amount of thrust produced. FAST's regressions support this, predicting a single engine weight lower than the combined weight of the two engines on the baseline 737-8 Max (as reported in [21]), while delivering greater overall thrust (including both jet and electric thrust). A quantitative comparison is shown in Tab. 4. It is assumed that

integrating the propulsion system into the airframe and using electric propulsors with powertrain efficiencies greater than those of mechanical powertrains would yield weight benefits over FAST's prediction. However, without these assumptions declared, the benefits are neither quantifiable nor repeatable in this study.

Table 4 Engine Comparisons between FAST, literature, and a conventional baseline. Total thrust includes both gas turbine and electric thrust, as SUSAN's electric propulsors still on gas turbine power.

Parameter	787Max-8 [21]	Literature [21]	FAST
Number of Gas Turbines	2	1	1
System Weight (lbf)	14,470	7,520	10,272
Total Thrust Produced (lbf)	54,300	56,885	56,337

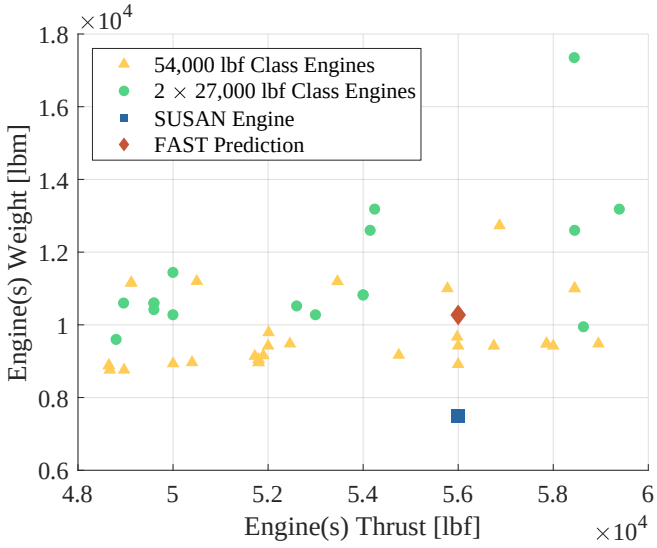

Fig. 7 Historical engine weight vs SLS thrust with SUSAN [21] and FAST [28] predicitions.

E. Engine Performance Modeling

To model turbofan engine performance in FAST, an empirical equation is used to rapidly compute the TSFC and fuel flow for a given flight condition [19]. A limitation of this equation is that it applies to conventional jet engines outside of an EAP system. However, SUSAN is a partially turboelectric aircraft. Therefore, the fuel flow equation provided in FAST must be generalized for conventional and EAP systems.

To improve the fuel flow estimation, an "equivalent thrust", T_{eqv}, must be estimated, which represents the thrust that is generated by the turbofan engine only. This quantity is derived from the output thrust, T_{output}, which is unique for each EAP system. This is exemplified by Fig. 8, which illustrates the output and equivalent thrusts for a parallel hybrid, series hybrid, and partially turboelectric propulsion systems. Once the equivalent thrust is derived for the EAP system at-hand, the fuel flow equation within FAST can be used to assess the turbofan's performance.

In conventional aircraft, the output and equivalent thrusts are equal, because there are no electrified systems supplementing or siphoning power. In parallel and series hybrid configurations, a portion of the thrust comes from the batteries or electric motors. These contributions must be subtracted to compute the equivalent thrust, which will be less than the output thrust. This is accomplished by traversing the propulsion system from the thrust sources to the downstream sources and subtracting the power contribution from each electrical component. Fig. 8 demonstrates this for the parallel and series hybrid propulsion architectures.

For SUSAN, which utilizes a partially turboelectric propulsion architecture, the equivalent thrust must account for the thrust generated by the aft fan and the DEP fans along the wing. In this case, the equivalent thrust is the sum of

the thrust from all these sources, adjusted by the efficiency of the electric motors and generators. This results in an equivalent thrust that is greater than the total thrust output. In other words, the turbofan engine must be sized to produce its own thrust, while also accounting for inefficiencies in the electrical powertrain, resulting in an equivalent thrust output that is greater than what would be seen in the exhaust of all of SUSAN's fans.

The framework proposed by Cinar et al. [27] is leveraged to compute the equivalent thrust for these disparate EAP systems. This allows the equivalent thrust to be computed using matrix operations rather than deriving an equivalent thrust expression for each EAP system.

Therefore, to accurately model the SUSAN concept using the engine performance equations from the FAST framework [19, 29], it is necessary to modify the required thrust, T, in the fuel flow rate equation to reflect the equivalent thrust, T_{eqv}, as calculated in Eq. 3. Additionally, the maximum static thrust, T_0, should be replaced with the maximum static thrust of the equivalent thrust, $T_{eqv,max}$. Eq. 4 shows the initial fuel flow equation[29] for conventional turbofan aircraft, and Eq. 5 presents the modified fuel equation for the SUSAN concept. Furthermore, Jansen et al. [2] identified the Boeing 737-8 Max equipped with two LEAP-1B25 engines as a baseline for the SUSAN concept. Consequently, this study employs a linear scaling factor of the fuel consumption rate of two LEAP-1B25 engines shown in Eq. 6 to obtain the necessary coefficients for the modified fuel flow equation based on the maximum thrust requirements.

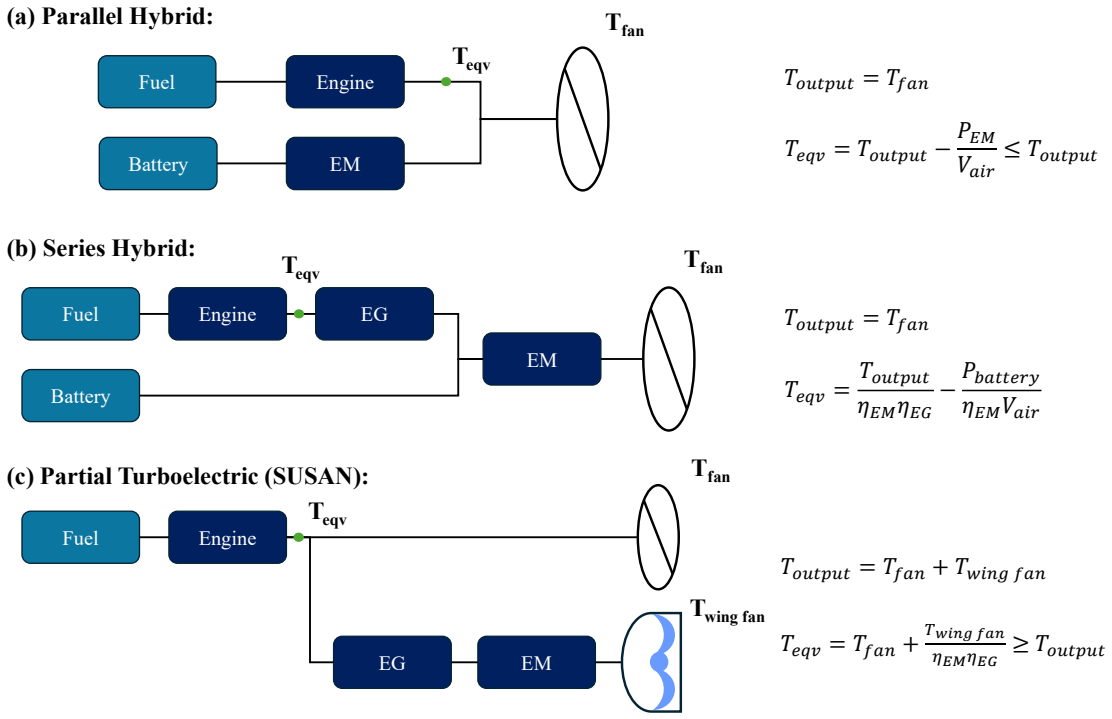

Fig. 8 The comparison of the equivalent thrust of a engine in different electrified aircraft propulsion architecture.

$$T_{eqv} = T_{fan} + \frac{T_{wingfan}}{\eta_{EM}\,\eta_{EG}} \tag{3}$$

$$\dot{m}_{f,initial}\,(T,h) = C_{ff3}\left(\frac{T}{T_{max}}\right)^3 + C_{ff2}\left(\frac{T}{T_{max}}\right)^2 + C_{ff1}\left(\frac{T}{T_{max}}\right) + C_{ff,ch} \times T \times h \tag{4}$$

$$\dot{m}_{f,modified}\,(T_{eqv},h) = a \times \left(C_{ff3}\left(\frac{T_{eqv}}{T_{eqv,max}}\right)^3 + C_{ff2}\left(\frac{T_{eqv}}{T_{eqv,max}}\right)^2 + C_{ff1}\left(\frac{T_{eqv}}{T_{eqv,max}}\right)\right) + C_{ff,ch} \times T_{eqv} \times h \tag{5}$$

$$a = \frac{T_{eqv,max}}{T_{LEAP-1B25,max}} \tag{6}$$

In these equations, $\dot{m}_f\left(T_{eqv}, h\right)$ represents the fuel flow rate of an engine (kg/s); C_{ff3}, C_{ff2}, and C_{ff1} represent the coefficients for the polynomial function (kg/s); $C_{ff,ch}$ represents the correlation factor for the cruise altitude condition $\left(\frac{kg}{s \times kN \times m}\right)$; T_{eqv}, $T_{eqv,max}$ and $T_{LEAP-1B25,max}$ represent the required equivalent thrust, the maximum static thrust of the engine and the maximum thrust of the LEAP1B-25 engine (kN), respectively; T_{fan} and $T_{wingfan}$ are the thrust from the aft fan and wing fan (kN); η_{EM} and η_{EG} are the efficiencies of the EMs and EGs; h_{CR} represents the cruise altitude of aircraft; and a is the linear scaling factor for the modified fuel flow rate, based on LEAP-1B25 engine performance.

F. Boundary Layer Ingestion (BLI) Effect

SUSAN's aft engine includes BLI technologies to reduce the fuel burn by increasing the propulsion system's efficiency or reducing the fuselage drag [30], as illustrated in Fig. 9. Secchi et al. indicated that the 1-D boundary layer thickness of turbulent flows is a function of Reynolds number and a correlation factor, f, as shown in Eq. 7 [31, 32]. The correlation factor is applied to modify the assumption that the turbulent flow is over a thin, one-dimensional flat plate (which assumes that the flow around the body is uniform). However, the fuselage is rounded and does not have a uniform flow around it.

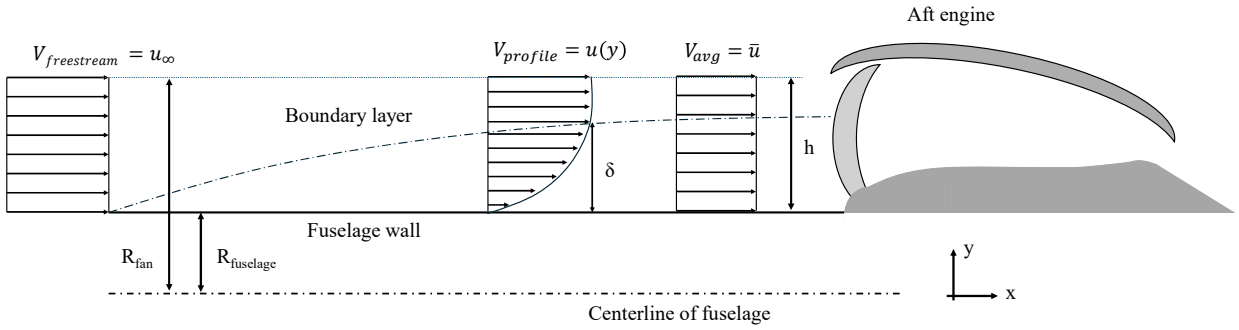

Fig. 9 The comparison of the equivalent thrust of a engine in different electrified aircraft propulsion architecture.

$$\frac{\delta}{x} = f\frac{0.382}{Re_x^{1/5}} \tag{7}$$

In Eq. 7, δ is the boundary layer thickness; x is the fuselage length; f is the correlation factor (1.24 for the cruise condition); and $Re_x^{1/5}$ is the flat plate Reynolds number characteristic length of the fuselage.

The power law velocity profile, known as 1/7$^{\text{th}}$ power law, is applied to model the turbulent velocity gradient arising from moderately favorable pressure gradients, as shown in Eq. 8. Once the height, y, is greater than the boundary layer thickness, the velocity will be equal to that of the freestream. At heights less than the boundary layer thickness, the average velocity profile follows the 1/7$^{\text{th}}$ power relation.

$$u(y) = u_\infty\left(\frac{y}{\delta}\right)^{1/7} \tag{8}$$

The average boundary layer flow velocity at the inlet of the nacelle is estimated by integrating the velocity profile along the boundary layer thickness, represented by Eq. 9. There are two possible conditions for the average flow velocity estimation. First, the nacelle height, h, is less than or equal to the boundary layer thickness ($h \leq \delta$). As a result, the fan can only ingest a portion of boundary layer. Second, the nacelle height, h, is greater than the boundary layer thickness ($h > \delta$) and the fan can ingest the entire boundary layer and a portion of freestream. Since turbulent flows have larger boundary layers, the turbulent flow over the fuselage reduces the size of the freestream layer that is ingested.

$$\overline{u} = \begin{cases} \frac{7}{8}u_\infty\left(\frac{h}{\delta}\right)^{1/7} & \text{if } h \leq \delta \\ u_\infty\left(-\frac{1}{8}\frac{1}{(h/\delta)} + 1\right) & \text{if } h > \delta \end{cases} \tag{9}$$

After accounting for BLI technologies in FAST, the engine performance model was validated for SUSAN's aft turbofan with and without BLI. This was done by only accounting for the 35% thrust that the aft fan generates. Relative

to the TSFC from literature [2], FAST predicts a TSFC with less than a 0.1% error, as indicated in Tab. 5. Therefore, the BLI model in FAST provides a reasonable estimation of the fuel consumption for the SUSAN's aft engine and can be used in further analyses.

Table 5 The validation of boundary layer ingestion function in FAST with the literature for 35% thrust split.

	Cruise TSFC in literature [9], $\frac{lbm}{lbf \cdot hr}$	Cruise TSFC in FAST, $\frac{lbm}{lbf \cdot hr}$	Difference
Non BLI for aft engine	0.4421	0.4420 III.D	+0.02%
With BLI for aft engine	0.4352	0.4351	-0.02%

G. Natural Laminar Flow Effect

Natural laminar flow (NLF) is also incorporated into SUSAN's design by adjusting the wing airfoil shape to provide beneficial pressure gradients that prevent crossflow and other aerodynamic instabilities [23]. The adjustments to the airfoil's thickness and camber are meant to prevent the flow from becoming turbulent, thus preventing increases in frictional drag. Lynde et al. [23] indicated that NLF is expected to reduce wing drag up to 8.8% and increase the lift-to-drag ratio by 9.6%. Results from the most recent NASA analyses, including that of Chau and Duensing [21], use a lift to drag ratio that includes the 9.6% increase due to NLF. The 9.6% lift to drag ratio increase was included in the SUSAN model.

IV. Results and Discussions

Using the technologies outlined in Section III, SUSAN was modeled in FAST and included BLI, DEP, and NLF effects. Using this model, an initial set of results are presented and compared to the results listed in NASA's 2024 update [21]. The implications of these results for wing and control surface sizing are also discussed.

A. Initial Aircraft Sizing Results

After running the initial SUSAN model in FAST, the OEW and airframe weight modeled in FAST were 6.4% and 5.0% smaller than the estimates from NASA, respectively. The fuel weight was overestimated by approximately 7.6% [21]. To reduce the error, calibration factors on the airframe weight, fuel flow rate, and cruise lift to drag ratio were used to closely match the block fuel, MTOW, and OEW provided in literature. These calibration factors are presented in Tab 6. After calibrating, the error in block fuel, MTOW, OEW, and airframe weight were all less than 3%.

Table 6 Calibration factors for the SUSAN model in FAST.

Calibration Factor	Value
Cruise L/D	1.02
Fuel Mass Flow Rate	0.947
Airframe Weight	1.052

Table 7 compares SUSAN's weights output by FAST relative to those found from NASA's previous efforts [21].Fig. 10 and Fig. 11 are output by FAST to visualize and rapidly assess SUSAN's performance throughout the mission. Additional fuel flow and power profile results can be found in Fig.s 13 and 14 in Appendix VII.A. After analyzing SUSAN in FAST, its MTOW is 189,394 lbs, with an OEW of 117,460 lbs and an airframe weight estimate of 79,449 lbs. The aircraft has a block fuel requirement of 30,701 lbs, which is a 28% improvement over the fuel burn for the Boeing 737-8 Max aircraft based on the NASA research [21]. This equates to approximately 11,000 lbs of fuel saved over the design mission without sacrificing payload.

Fig. 10 and Fig. 11 indicate that SUSAN requires about 28.7 MW of power at takeoff and 8.94 MW of power at cruise, for an approximate cruise TSFC of 0.4732 lbm/(lbf*hr). After applying the thrust split and assuming that the electric motors will act as power sources to provide 65% of the power required by the DEP systems, the total requirements at cruise and takeoff are 5.8 MW and 18.6 MW, respectively. These are within the 10 MW and 20 MW power load limits set by NASA [21]. However, there remain sizing differences between the engine model used in FAST

Table 7 Comparing sized outputs for the SUSAN model from FAST to the weight table published by NASA.

Weight Group	FAST (lbs)	NASA (lbs) [21]	Error (%)
MTOW	189,394	190,890	-0.63
OEW	117,460	120,950	-2.89
Airframe	79,449	79,370	+0.10
Payload	39,710	39,600	+0.28
Block Fuel	30,701	30,340	+1.19
Electric Motor	3,309	4,700	-29.59
Engine	10,295	7,520	+36.90

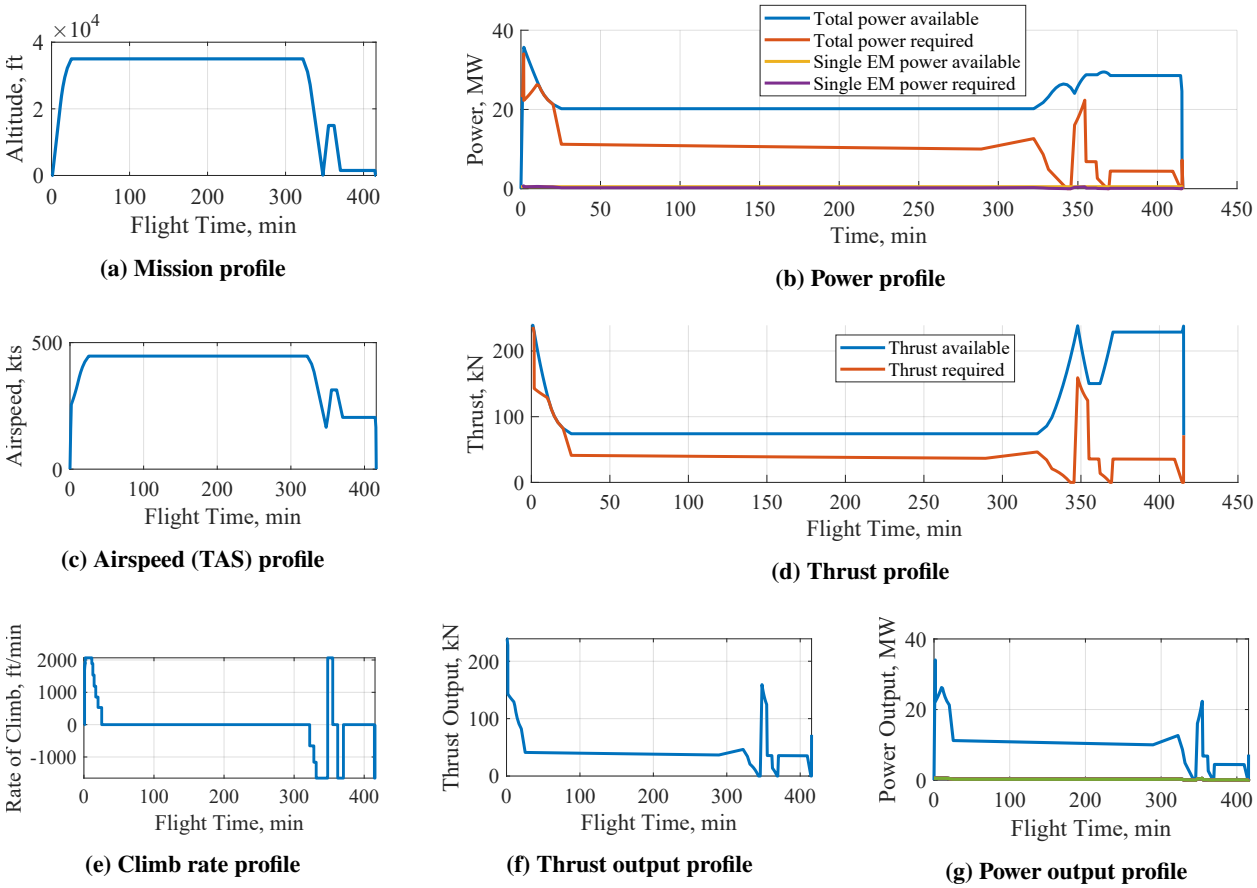

(a) Mission profile

(b) Power profile

(c) Airspeed (TAS) profile

(d) Thrust profile

(e) Climb rate profile

(f) Thrust output profile

(g) Power output profile

Fig. 10 The thrust and power profiles for the SUSAN model resulting from the mission profile analysis in FAST.

and that designed by NASA, particularly as discussed in Section III.D. The largest sources of error are the engine and electric propulsor weights, which deviate from their literature values by 36.9% and 29.6%, respectively. This is likely due to the propulsion system simplifications and differences in how the engine sizing estimates are made between this work and NASA's study.

Some subsystems that are not considered in FAST were sized in the NASA analyses, such as the thermal management systems [21]. Furthermore, some components such as the electric wiring make up a significant portion of the weight, but were roughly estimated after making several assumptions. The complexity and scope of these estimates makes them prohibitively difficult to replicate exactly – some error is expected. Also, FAST's regressions fill in the engine specifications based on data from previously built engines, while the NASA engine deck is based on future technology assumptions.

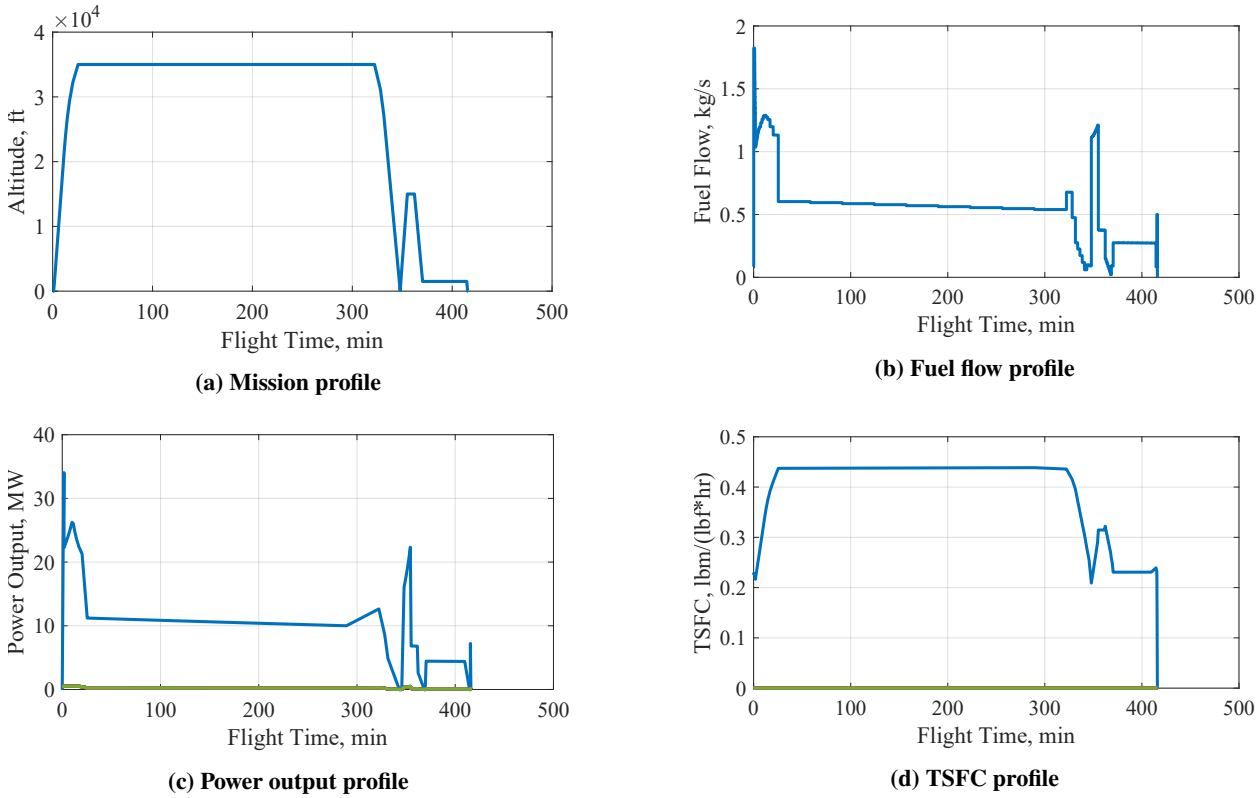

(a) Mission profile

(b) Fuel flow profile

(c) Power output profile

(d) TSFC profile

Fig. 11 Fuel flow, power output and TSFC profiles for the SUSAN model resulting from analysis of the mission profile in FAST.

Despite these modeling differences, the results are sufficiently accurate to comparatively evaluate the sizing and performance benefits of different advanced technologies on SUSAN's design. The errors identified here are carried throughout experimentation, and should not affect the model behavior as advanced technologies continue to be added into the aircraft.

B. SUSAN Aircraft Visualization and Sizing Implications

In addition to the aircraft sizing and mission analyses, FAST can produce a scaled visualization of the aircraft using simple but generic components [33]. A visualization of SUSAN is provided in Fig. 12. The aircraft components are scaled based on the sizing results, and match what an actual aircraft would look like if it was manufactured to enter into service. This provides a quick, top-level confirmation that the SUSAN model outputs are physically reasonable.

Significant work is needed to evaluate the control surface sizing modifications from adding advanced technologies into SUSAN's design. However, some elementary predictions can be made based on the results presented thus far. FAST predicted SUSAN's lift to drag ratio was 20.49, approximately 4% and 14% larger than the values predicted by NASA for its SUSAN studies and the Boeing 737-8 Max, respectively [21]. This means that the aircraft wing with DEP is more efficient, and does not require as large a lifting force contribution from the tail or flaps at takeoff. The high lift to drag ratio also indicates a larger maximum lift coefficient, which is expected for DEP systems and reduces the dependency on flaps for high lift during takeoff [22, 24]. Furthermore, FAST predicts a wing area of 1,461 ft^2, which is a 4.7% increase in the wing size relative to the Boeing 737-8 Max [21]. This is significant because the tail volume coefficients can be reduced, leading to a smaller tail, minor weight reductions, reduced parasite drag, and potentially reduced dependency on control surfaces at the tail.

The tail volume coefficient may also be reduced as a result of the turbofan engine being moved from to the tail. According to Raymer, this may yield as much as a 5-10% reduction in the moment arm between the tail and wing [34], consequently decreasing the surface area necessary at the tail to counteract destabilizing moments produced by an engine failure. Overall, these results are encouraging and indicate that SUSAN aircraft may have a reduced dependency

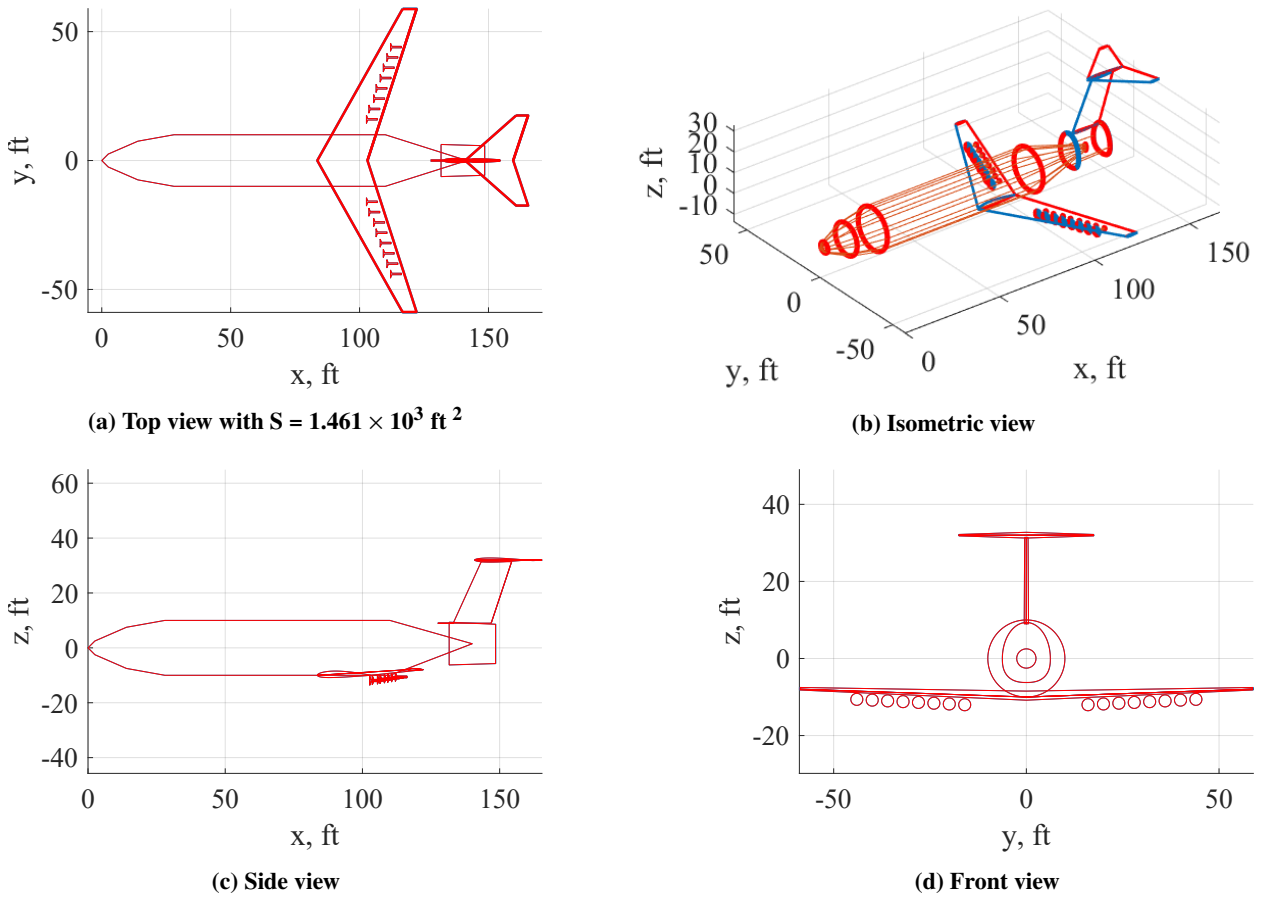

(a) Top view with S = 1.461 × 10^3 ft ^{2}

(b) Isometric view

(c) Side view

(d) Front view

Fig. 12 SUSAN visualization produced by FAST, scaled to the sizing and performance parameters.

on the tail's control surfaces, particularly those on the vertical tail. Additional analysis must be completed to determine how DEP may further reduce the reliance on standard control surfaces and whether or not the thrust sources in a DEP system can replace or supplement the functionality of the primary control surfaces.

V. Conclusion

To reduce CO_2 emissions by 2050 and meet the rising demand for electrification in commercial aviation, NASA proposed the SUSAN electrofan concept. This vehicle utilizes a novel partially turboelectric propulsion system with a single turboshaft engine driving an aft-mounted fan and 32 ducted fans distributed along the wings. It harnesses advanced technologies such as BLI, NLF, and advanced propulsion-airframe integration to reduce fuel burn. These technologies were integrated under one, comprehensive model and assessed using FAST. The resulting aircraft has an MTOW of 189,394 lbs and a block fuel of 30,701 lbs. The vehicle requires 28.7 MW of power from the engine at takeoff, but only 8.94 MW at TOC. A high L/D of 20.49 indicates that DEP systems may serve to reduce dependencies on traditional control surfaces in previously unexplored ways. Validation of the BLI technology modeled in this work further illustrated the potential for that technology to reduce aft-mounted engine's fuel burn. Overall, these preliminary results indicate that SUSAN is capable of meeting the design goals set forth by NASA, and encourage further investigation into the role that EAP systems can play to reduce commercial aviation's environmental impact. Work with the SUSAN model will continue to explore how distributed propulsion systems can be used in novel ways to decrease the reliance on traditional control surfaces.

VI. Future Work

The next steps to better model SUSAN involve eliminating the propulsion system simplifications as well as more accurately sizing individual components for the reserve missions. Work is underway to improve FAST such that it can model propulsion architectures with three consecutive power sources. This will allow the electric generators and motors to be sized independently and lend itself to a more granular analysis. To meet the off-design mission requirements, the electric propulsors will be resized to provide the total thrust required in the event of an aft-fan failure, which should resolve sizing discrepancy within that weight group. Additionally, the batteries will be sized based on the power requirements for the reserve mission, since they are designed to provide the necessary power to the electric propulsors in the event of an engine failure or loss of fuel. A redundancy impact analysis will also be completed to establish the trade-offs between redundancy in the propulsion system and the weight of the propulsion system components. This trade-off will impact the system safety and certification of SUSAN as well as its overall performance with heavier propulsion system components.

Following this, a baseline model of SUSAN without any BLI or NLF effects will be developed in FAST to evaluate what impact these technologies have on the aircraft efficiency and power required. The impacts of DEP on the aircraft's dynamics during takeoff will be determined, especially the potential for supplementing the takeoff thrust such that the aft engine can be sized for cruise, a less power demanding design condition. There will also be a focus on control surface sizing between the two models to determine how the novel propulsion system and advanced technologies impact the aircraft's dependency on traditional wing and tail control surfaces. The ramifications of any control surface sizing reduction will be evaluated with respect to the aircraft's system architecture and overall performance and efficiency. These analyses will include a consideration of how changes to traditional control surface sizing may impact aircraft safety.

VII. Appendix

These appendices provide additional results and context for the development of the SUSAN model. VII.A contains the power and fuel profiles for the SUSAN mission profile and performance analysis. VII.B provides the EAP system component weight breakdown used to develop the EAP weight variable for the initial estimates used in the SUSAN aircraft specifications file.

A. FAST Sizing Results

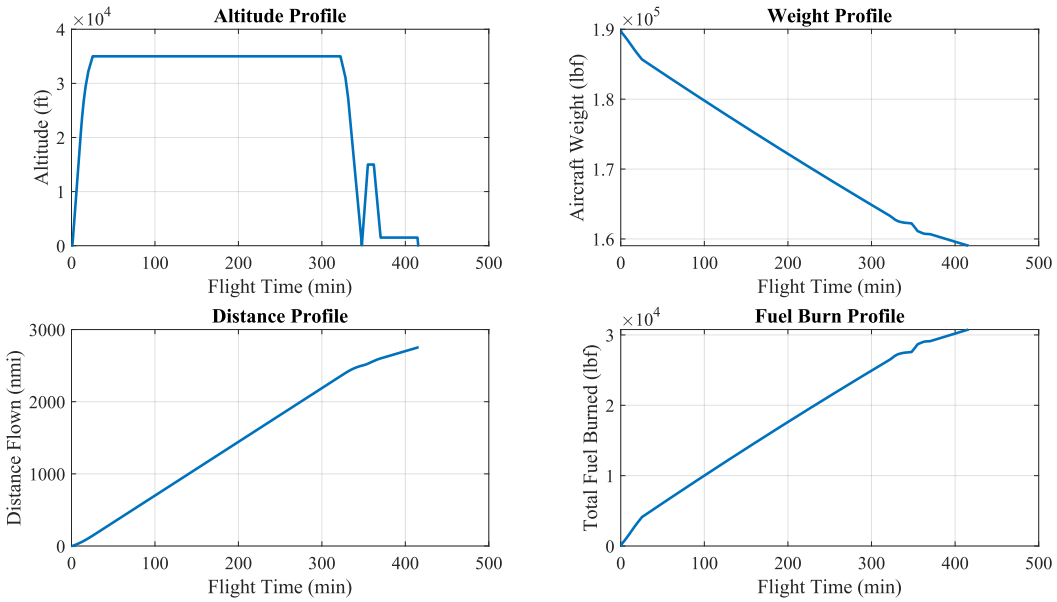

Fig. 13 The fuel burn and weight profile results for the FAST analysis of the SUSAN electrofan model.

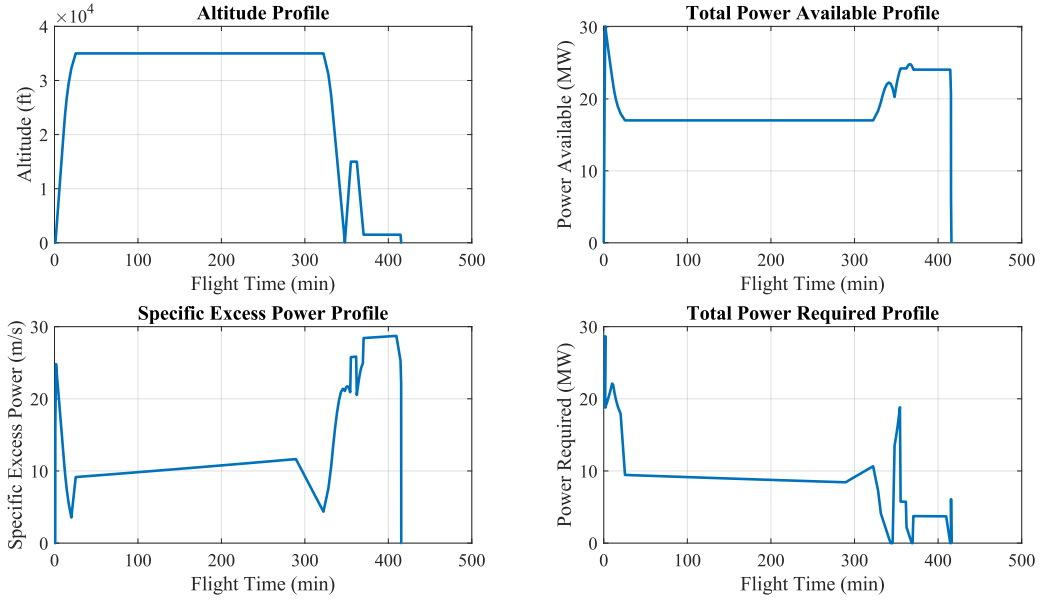

Fig. 14 The power profile results for the FAST analysis of the SUSAN electrofan model.

B. EAP Component Weight Table

Table 8 The component weight table used to calculate and organize the EAP system weight component, based on information from Chau et al [21].

EAP Systems	kW/kg	kW per item	Number	kW total	Efficiency	lbs
Main Generators						
Electric Propulsors						
Main Generator	25	5000	4	20000	99.00%	1777.78
Power Systems						
AC Circuit Interrupters	300	1250	16	20000	99.50%	1777.78
HP Shaft Motor						
Electric Propulsors						
Turbine Control M/G	20	1000	1	1000	99.00%	111.11
Power Systems						
Turbine C Converter	15	250	4	1000	98.00%	149.66
AC Circuit Interrupters	300	250	4	1000	99.50%	7.37
Electric Wing Engines						
Electric Propulsors						
Electric Engine Motor	20	800	32	25600	98.50%	2858.88
Power Systems						
Main Gen Converter	30	1500	16	24000	99.00%	1777.78
Electric EM Converter	20	600	32	19200	99.00%	2133.33
Battery Converter	10	1250	16	20000	98.00%	4489.8
AC Circuit Interrupters	300	600	32	19200	99.50%	141.51
DC Circuit Interrupters	150	125	32	4000	99.50%	58.96
Battery Systems						
Single Use	1500	450000	16	7200000		10560
Rechargeable	500	10417	16	166667		733.33
Thermal Systems						2580
Total EAP System Weight						29157.3

Table 9 Total subsystem weights based on the component table.

Subsystem	Component Weight Total (lbs)
Electric Propulsors	4747.77
Power Systems	10536.18
Thermal Systems	2580
Battery Systems	11293.33

Funding Sources

This work is sponsored by the NASA Aeronautics Research Mission Directorate and Electrified Powertrain Flight Demonstration project, "Development of a Parametrically Driven Electrified Aircraft Design and Optimization Tool", WO-0238.

Acknowledgments

The authors would like to thank Ralph Jansen, Amy Chicatelli, Andrew Meade, Karin Bozak, Noah Listgarten, Dennis Rohn, and Gaudy Bezos-O'Connor from NASA's Electrified Powertrain Flight Demonstration project for supporting this work and providing valuable technical input and feedback throughout the duration of the project. The authors also thank Huseyin Acar, Rawan Aljaber, Swapnil Jagtap, Nawa Khailany, Janki Patel, Joaquin Rey, Jayda Shine, and Michael Tsai for their contributions to FAST, including the regressions; visualization package; and engine modeling that the SUSAN model depends on.

References

[1] Federal Aviation Administration, "2021 United States Aviation Climate Action Plan," , 2021. URL https://www.faa.gov/sites/faa.gov/files/2021-11/Aviation_Climate_Action_Plan.pdf.

[2] Jansen, R., Kiris, C. C., Chau, T., Machado, L. M., Duensing, J. C., Mirhashemi, A., Chapman, J., French, B. D., Miller, L., Litt, J. S., et al., "Subsonic single aft engine (SUSAN) transport aircraft concept and trade space exploration," *AIAA SciTech 2022 Forum*, 2022, p. 2179. https://doi.org/10.2514/6.2022-2179.

[3] Jansen, R. H., Kiris, C. C., Chau, T., Machado, L., Dever, T. P., Litt, J. S., Arthur, J. J., Lynde, M. N., Chapman, J. W., Kratz, J. L., et al., "Update on SUbsonic Single Aft eNgine (SUSAN) Electrofan Trade Space Exploration," *33rd Congress of the International Council of the Aeronautical Sciences*, 2022. URL https://www.icas.org/ICAS_ARCHIVE/ICAS2022/data/papers/ICAS2022_0774_paper.pdf.

[4] Mirhashemi, A., Chapman, J., Miller, C., Julia, S., and Jansen, R., "Tail-mounted engine Architecture and Design for the Subsonic Single Aft Engine Electrofan Aircraft," *AIAA SciTech 2022 Forum*, 2022, p. 2182. https://doi.org/10.2514/6.2022-2182.

[5] NASA Glenn Researcher Center, "Subsonic Single Aft Engine (SUSAN) Aircraft," , 2023. URL https://www1.grc.nasa.gov/aeronautics/eap/airplane-concepts/susan/.

[6] Yildirim, A., Gray, J. S., Mader, C. A., and Martins, J. R., "Performance analysis of optimized STARC-ABL designs across the entire mission profile," *AIAA SciTech 2021 Forum*, 2021, p. 0891. https://doi.org/10.2514/6.2021-0891.

[7] Machado, L. M., Chau, T., Kenway, G. K., Duensing, J. C., and Kiris, C. C., "Preliminary Assessment of a Distributed Electric Propulsion System for the SUSAN Electrofan," *AIAA SciTech 2023 Forum*, 2023, p. 1748. https://doi.org/10.2514/6.2023-1748.

[8] Denham, C. L., Chau, T., Ryan, W., and Jansen, R., "Mission Profiles for the SUSAN Electrofan Concept," *AIAA SciTech 2023 Forum*, 2023, p. 1938. https://doi.org/10.2514/6.2023-1938.

[9] Chapman, J. W., Kratz, J. L., Dever, T., Mirhashemi, A., Heersema, N., and Jansen, R., "SUSAN Concept Vehicle Power and Propulsion System Study," *AIAA SciTech 2023 Forum*, 2023, p. 1749. https://doi.org/10.2514/6.2023-1749.

[10] Chapman, J. W., "Considering Turbofan Operability in Hybrid Electric Aircraft Propulsion System Design," *AIAA SCITECH 2023 Forum*, 2023, p. 2178. https://doi.org/10.2514/6.2023-2178.

[11] Jansen, R. H., Kascak, P., Dyson, R., Woodworth, A., Scheidler, J., Smith, A. D., Stalcup, E., Tallerico, T., de Jesus-Arce, Y., Avanesian, D., Duffy, K., Passe, P., and Szpak, G., "High Efficiency Megawatt Motor Preliminary Design," *2019 AIAA/IEEE Electric Aircraft Technologies Symposium (EATS)*, 2019, pp. 1–13. https://doi.org/10.2514/6.2019-4513.

[12] Jansen, R., De Jesus-Arce, Y., Kascak, P., Dyson, R. W., Woodworth, A., Scheidler, J. J., Edwards, R., Stalcup, E. J., Wilhite, J., Duffy, K. P., et al., "High efficiency megawatt motor conceptual design," *2018 Joint Propulsion Conference*, 2018, p. 4699. https://doi.org/10.2514/6.2018-4699.

[13] Granger, M., Anderson, A., Maroli, J. M., Tallerico, T., and Scheidler, J. J., "Combined Analysis of NASA's High Efficiency Megawatt Motor and Its Converter," *2021 AIAA/IEEE Electric Aircraft Technologies Symposium (EATS)*, 2021, pp. 1–13. https://doi.org/10.23919/EATS52162.2021.9704834.

[14] NASA Glenn Researcher Center, "HEATheR Activity," , 2021. URL https://www1.grc.nasa.gov/aeronautics/eap/technology/heather/.

[15] NASA Glenn Researcher Center, "Converters," , 2023. URL https://www1.grc.nasa.gov/aeronautics/eap/technology/converters/.

[16] Dever, T. P., and Jansen, R. H., "Cable Key Performance Parameters for Megawatt Electrified Aircraft Propulsion Conceptual Aircraft Model," *2022 IEEE Transportation Electrification Conference Expo (ITEC)*, 2022, pp. 748–753. https://doi.org/10.1109/ITEC53557.2022.9814005.

[17] Brady, C., "The Boeing 737 Technical Guide," , 2023. URL http://www.b737.org.uk/techspecsdetailed.htm.

[18] Eller, A., "Energy and Power of Flying," , 2013. URL http://large.stanford.edu/courses/2013/ph240/eller1/.

[19] Mokotoff, P., Maxfield, A., Wang, Y.-C., and Gokcin, C., "FAST: A Future Aircraft Sizing Tool for Electrified Aircraft Design," *AIAA SciTech 2025 Forum*, 2025. The abstract is submitted subject to peer review.

[20] Maxfield, A., Rawan, A., and Gokcin, C., "Perdiciting Aircraft Design Parameters Using Gaussian Process Regression on Historical Data," *AIAA SciTech 2025 Forum*, 2025. The abstract is submitted subject to peer review.

[21] Chau, T., and Duensing, J., "Conceptual Design of the Hybrid-Electric Subsonic Single Aft Engine (SUSAN) Electrofan Transport Aircraft," *AIAA SCITECH 2024 Forum*, 2024, p. 1326. https://doi.org/10.2514/6.2024-1326.

[22] Lee, B. J., and Liou, M.-F., "Conceptual Design of Propulsors for the SUSAN Electro-fan Aircraft," *AIAA SciTech 2022 Forum*, 2022, p. 2305. https://doi.org/10.2514/6.2022-2305.

[23] Lynde, M. N., Campbell, R. L., and Hiller, B. R., "A Design Exploration of Natural Laminar Flow Applications for the SUSAN Electrofan Concept," *AIAA Scitech 2022 Forum*, 2022, p. 2303. https://doi.org/10.2514/6.2022-2303.

[24] Chau, T., Kenway, G., and Kiris, C. C., "Conceptual Exploration of Aircraft Configurations for the SUSAN Electrofan," *AIAA SciTech 2022 Forum*, 2022, p. 2181. https://doi.org/10.2514/6.2022-2181.

[25] Federal Aviation Administration, "91.117 Aircraft Speed," , 2024. URL https://www.ecfr.gov/current/title-14/section-91.117.

[26] Federal Aviation Administration, "ENR 1.5 Holding, Approach, and Departure Procedures," , 2024. URL https://www.faa.gov/air_traffic/publications/atpubs/aip_html/part2_enr_section_1.5.html.

[27] Cinar, G., Garcia, E., and Mavris, D. N., "A framework for electrified propulsion architecture and operation analysis," *Aircraft Engineering and Aerospace Technology*, Vol. 92, No. 5, 2020, pp. 675–684. https://doi.org/10.1108/AEAT-06-2019-0118.

[28] Maxfield, A., Rawan, A., and Gokcin, C., "Predicting Aircraft Design Parameters using Gaussian Process Regressions on Historical Data," *AIAA SciTech 2025 Forum*, 2025. This paper is currently under review and has not been accepted yet.

[29] Sun, J., Hoekstra, J. M., and Ellerbroek, J., "OpenAP: An open-source aircraft performance model for air transportation studies and simulations," *Aerospace*, Vol. 7, No. 8, 2020, p. 104.

[30] Blumenthal, B., Elmiligui, A. A., Geiselhart, K., Campbell, R. L., Maughmer, M. D., and Schmitz, S., "Computational investigation of a boundary layer ingestion propulsion system for the common research model," *46th AIAA Fluid Dynamics Conference*, 2016, p. 3812. https://doi.org/10.2514/6.2016-3812.

[31] Secchi, M., Lacava, P. T., Trapp, L. G., and Gama Ribeiro, R. F., "Evaluation of a Regional Aircraft with Boundary Layer Ingestion and Electric-Fan Propulsor," *Journal of Aircraft*, Vol. 58, No. 6, 2021, pp. 1204–1215. https://doi.org/10.2514/1.C035932.

[32] Schlichting, H., and Gersten, K., *Boundary-layer theory*, springer, 2016.

[33] Khailany, N., Mokotoff, P., and Gokcin, C., "Aircraft Geometry and Propulsion Architecture Visualization for the Future Aircraft Sizing Tool (FAST)," *AIAA SciTech 2025 Forum*, 2025. The abstract is submitted subject to peer review.

[34] Raymer, D. P., *Initial Sizing*, American Institute of Aeronautics and Astronautics, 1992, pp. 101–116.